Water Research 194 (2021) 116964

Contents lists available at ScienceDirect

Water Research

journal homepage: www.elsevier.com/locate/watres

Formation and control of C- and N-DBPs during disinfection of filter backwash and sedimentation sludge water in drinking water treatment

Yunkun Qian[a], Yanan Chen[a], Yue Hu[a], David Hanigan[b], Paul Westerhoff[c], Dong An[a,d,*]

[a] Department of Environmental Science & Engineering, Fudan University, Shanghai 200238, PR China
[b] School of Sustainable Engineering and the Built Environment, Ira A. Fulton Schools of Engineering, Arizona State University, Tempe, AZ, 85287-3005, USA
[c] Department of Civil and Environmental Engineering, University of Nevada, Reno, NV, 89557-0258, USA
[d] Shanghai Institute of Pollution Control and Ecological Security, Shanghai 200092, PR China

ARTICLE INFO

Article history:
Received 6 December 2020
Revised 4 February 2021
Accepted 22 February 2021
Available online 23 February 2021

Keywords:
disinfection byproducts
Filter backwash water
sedimentation sludge water
Calculated toxicity

ABSTRACT

Drinking water treatment plants (DWTPs) produce filter backwash water (FBW) and sedimentation sludge water (SSW) that may be partially recycled to the head of DWTPs. The impacts of key disinfection conditions, water quality parameters (e.g., disinfection times, disinfectant types and doses, and pH values), and bromide concentration on controlling the formation of trihalomethanes (THMs), haloacetic acids (HAAs), haloacetonitriles (HANs), and haloacetamides (HAMs) during disinfection of FBW and SSW were investigated. Concentrations of most disinfection byproducts (DBPs) and associated calculated toxicity increased with extended chlorination for both FBW and SSW. During chlorination of both FBW and SSW, elevated chlorine doses significantly increased THM yields per unit dissolved organic carbon (DOC), but decreased HAN and HAM yields, with minimum effect on HAA yields. Chloramine disinfection effectively inhibited C-DBP formation but promoted N-DBPs yields, which increased with chloramine dose. Calculated toxicities after chloramination increased with chloramine dose, which was opposite to the trend found after free chlorine addition. An examination of pH effects demonstrated that C-DBPs were more readily generated at alkaline pH (pH=8), while acidic conditions (pH=6) favored N-DBP formation. Total DBP concentrations increased at higher pH levels, but calculated DBP toxicity deceased due to lower HAN and HAM concentrations. Addition of bromide markedly increased bromo-THM and bromo-HAN formation, which are more cytotoxic than chlorinated analogues, but had little impact on the formation of HAAs and HAMs. Bromide incorporation factors (BIFs) for THMs and HANs from both water samples all significantly increased as bromide concentrations increased. Overall, high bromide concentrations increased the calculated toxicity values in FBW and SSW after chlorination. Therefore, while currently challenging, technologies capable of removing bromide should be explored as part of a strategy towards controlling cumulative toxicity burden (i.e., hazard) while simultaneously lowering individual DBP concentrations (i.e., exposure) to manage DBP risks in drinking water.

1. Introduction

Disinfection is the primary operation for ensuring the biosafety of drinking water that is used in drinking water treatment plants and prevents transmission of illness by water (Richardson et al., 2007; Shannon et al., 2008). A now predictable consequence of disinfection is the reaction of the chemical oxidants (e.g., free chlorine, chloramines) with natural organic matter in water to form disinfection byproducts (DBPs), some of which are potential or known human carcinogens and cause bladder and colon cancer (Cantor et al., 2010; Costet et al., 2011; Rahman et al., 2010; Villanueva et al., 2004, 2006). Approximately 600–700 DBPs, including carbonaceous DBPs (C-DBPs, e.g., trihalomethanes (THMs), haloacetic acids (HAAs)) and nitrogenous DBPs (N-DBPs, e.g., nitrosodimethylamine, haloacetonitriles (HANs), and haloacetamides (HAMs)), have been detected in treated waters (An et al., 2019; Chen et al., 2010; Hanigan et al., 2015; Krasner et al., 2018; Vu et al., 2018). With the development of high sensitivity instruments and sensitive toxicity screening assays, N-DBPs have been detected in drinking water and potentially pose orders of magni-

* Corresponding author.
E-mail address: andong@fudan.edu.cn (D. An).

https://doi.org/10.1016/j.watres.2021.116964
0043-1354/

tude greater toxicity than C-DBPs (Bond et al., 2011; Krasner et al., 2013; Lau et al. 2020; Plewa et al., 2017).

Many countries have established maximum contamination levels for some of DBPs in finished water to reduce the potential adverse effects on human health (Chuang et al., 2019; Zeng et al., 2016). The United States Environmental Protection Agency (USEPA) regulates the sum of four THMs at 80 μg/L and 60 μg/L for five HAAs (US EPA, 2006). In China, the maximum concentrations of individual THMs (trichloromethane (TCM), bromodichloromethane (BDCM), dibromochloromethane (DBCM), and tribromomethane (TBM)) in finished water must not exceed 60, 60, 100, and 100 μg/L, respectively, and the sum of the ratios of the detected concentrations and their maximum concentrations must not exceed 1 (Standardization Administration of the People's Republic of China, 2006). A guideline value of 100 ng/L was adopted for maximum nitrosodimethylamine concentrations by the World Health Organization (WHO), while the state of California and other jurisdictions limits nitrosodimethylamine to 10 ng/L (California Department of Public Health, 2013; Massachusetts Office of EEA, 2004; WHO, 2008). However, there are many DBPs which remain unregulated, such as HANs and HAMs, which are more toxic than THMs and HAAs (Wagner and Plewa, 2017). Therefore, corresponding strategies should be applied to control DBP formation in finished water to reduce the health risks.

Chlorine is the most commonly used disinfectant due to its low cost and ability to effectively inactivate microorganisms and viruses. However, large numbers of C-DBPs (e.g., TCM, BDCM and dichloroacetic acid (DCAA)) are produced when chlorine is used as a disinfectant (Sedlak and Gunten, 2011). Therefore, many DWTPs have used alternative disinfectants such as chloramines, which reduced formation of C-DBPs compared to chlorine (Hua and Reckhow, 2007). However, chloramines increase the formation of some N-DBPs, which also tend to exhibit greater toxicity than the currently regulated C-DBPs (Guay et al., 2005; Hanigan et al., 2017; Wagner and Plewa, 2017). Previous studies have shown that Chinese hamster ovary cell cytotoxicity and genotoxicity of unregulated N-DBPs were 1–3 orders of magnitude higher than those of the regulated C-DBPs (Plewa et al., 2008, 2017). Therefore, N-DBPs are often the driver of toxicity among the DBPs measured, despite being present at low concentrations in finished water (Muellner et al., 2007; Verdugo et al., 2020).

Water resources are strained due to population growth and increased pollution. Therefore, DWTPs attempt to maximum internal plant recycling of wash- and waste-water flows. Filter backwash water (FBW) and sedimentation sludge water (SSW) are being considered as raw water sources for DWTPs (Hong et al., 2016; King et al., 2020). FBW and SSW produced during water treatment account for approximately 2–10% of total water flow in DWTPs (Gottfried et al., 2008). Therefore, recycling FBW and SSW not only reduces the costs of treatment and transportation but also increases net water production rates in DWTPs (Bourgeois et al., 2004; Krasner et al., 2009). However, we have recently shown that FBW and SSW contain large quantities of DBPs and precursors which result in the formation ofTHMs, HAAs, HANs and HAMs when chlorinated (Qian et al., 2020). A recent study also showed that nitrosamines were produced during recycling of settled sludge supernatant due to polymer residue (Westerhoff et al., 2019). FBW and SSW had high levels of bromide, with concentrations of 105–214 μg/L and 160–885 μg/L, respectively, in our previous study (Qian et al., 2020) and bromide enhances formation of higher toxicity bromo-DBPs (Krasner et al., 2016; Plewa et al., 2008 and 2010). While the effects of these disinfection conditions and water quality parameters on DBP formation have been extensively studied in surface water (Hong et al., 2013; Yang et al., 2007), little is known regarding the formation of DBPs during FBW and SSW recycling.

The objective of this research was to determine the effects of disinfection conditions (i.e., contact time, disinfectant chemistry, and dose) and water quality parameters (i.e., pH and bromide) on the formation of C- and N-DBPs during FBW and SSW recycling. The formation of four THMs, nine HAAs, seven HANs and six HAMs was measured, and cytotoxicity was calculated using published potency data. The results of this study are expected to provide useful information for controlling C- and N-DBP formation during of FBW and SSW recycling.

2. Materials and methods

2.1. Water sample collection

Water samples in this study consisted of sand filter backwash water (FBW) and sedimentation sludge water (SSW) that were collected from a typical drinking water treatment plant with a conventional treatment process, including coagulation, sedimentation, filtration and disinfection. The water source was the Qingcaosha Reservoir which is located in southern China. FBW and SSW were collected from the overflow of a gravity thickener which treated the filter backwash water and sedimentation sludge. Sodium thiosulfate was immediately added to the collected water samples to quench any residual chlorine. All samples were filtered with a 0.45 µm glass fiber filter and were then stored at 4°C in ice boxes until use. The water quality characteristics of the FBW and SSW are listed in Table S1.

2.2. Chemical reagents

C- and N-DBPs (e.g., THMs, HAAs, HANs and HAMs) in FBW and SSW were investigated in this study. Pure DBP standards in solvents were purchased from Dr. Ehrenstorfer (Augsburg, Germany). The THMs included TCM, DBCM, DBCM, and TBM. The HAAs included chloroacetic acid (CAA), bromoacetic acid (BAA), DCAA, trichloroacetic acid (TCAA), bromochloroacetic acid (BCAA), and dibromoacetic acid (DBAA), bromodichloroacetic acid (BDCAA), chlorodibromoacetic acid (CDBAA), and tribromoacetic acid (TBAA). The HANs included chloroacetonitrile (CAN), bromoacetonitrile (BAN), dichloroacetonitrile (DCAN), bromochloroacetonitrile (BCAN), trichloroacetonitrile (TCAN), dibromoacetonitrile (DBAN), and iodoacetonitrile (IAN). The HAMs included 2-chloroacetamide (CAM), 2-bromoacetamide (BAM), dichloroacetamide (DCAM), bromochloroacetamide (BCAM), trichloroacetamide (TCAM), and dibromoacetamide (DBAM). Methyl *tert*-butyl ether (MTBE, high performance liquid chromatography (HPLC) grade) was purchased from Sigma Aldrich (St. Louis, MO, USA). Ultrapure water was prepared using a Gradient A10 ultrapure water system (Milli-Q®, Millipore Corporation, Bedford, MA, USA). Anhydrous sodium sulfate (Na_2SO_4, analytical research grade, 99%) and other reagents (analytical grade) were obtained from the Sinopharm Chemical Reagent Co., Ltd. (Shanghai, China).

2.3. Experimental procedures

The roles of disinfectant contact time, disinfectant dose and chemistry, pH, and bromide concentration on THM, HAA, HAN, and HAM formations during FBW and SSW disinfection were investigated. Disinfection experiments were conducted in sealed 250 mL amber glass bottles at room temperature (25±1°C) in the dark. The disinfectant contact time and disinfectant (chlorine and chloramine) doses were 10–120 min and 5–20 mg-Cl_2/L, respectively, for simulating the disinfection process. pH of the water samples was adjusted to 6–8 with 2 mM phosphate buffer. The initial bromide concentrations in FBW and SSW were 0.05 and 0.42 mg/L,

respectively (Table S1). 0.1-1.0 mg/L bromide was added to investigate the effects of bromide concentration on DBP formations. The experimental processes were conducted in triplicate.

2.4. Analytical methods

Four THMs, seven HANs, six HAMs, and nine HAAs were measured using the modified EPA Methods 551.1 and 552.2 (US EPA, 1995, 2003). Briefly, separation and analysis was conducted via liquid-liquid extraction (LLE), followed by gas chromatography-electron capture detector (GC-ECD, 7890B, Agilent Technologies, USA) equipped with a 30 m × 0.25 mm × 0.25 μm DB-1701 column (J&W Scientific, USA). Detailed information on the analytical methods for DBPs are described in previously published procedures (An et al., 2017; Qian et al., 2020) and in the Supplemental Information.

Free chlorine was measured by the *N,N*-diethyl-*p*-phenylenediamine (DPD) powder pillow photometric method (APHA, 2005). Dissolved organic carbon (DOC) was measured using a total organic carbon (TOC) analyzer (Multi N/C 2100, Analytik Jena AG, Germany). Bromide was measured with a Finnigan ELEMENT XR double focusing magnetic sector field inductively coupled plasma (ICP)-MS instrument (Thermo Electron Corporation).

2.5. Calculations of bromide incorporation factors (BIFs) and cytotoxicity

Bromide incorporation factors (BIFs) indicate the proportion of bromine atoms incorporated into DBPs. BIFs were calculated according to previous research Jones et al., 2011; Petronijevic et al., 2019; Zhang et al., 2019) and Eqs. (1)-((4), in which all concentrations are on a molar basis.

$$BIF_{THMs} = \frac{C_{BDCM} + 2C_{DBCM} + 3C_{TBM}}{3C_{THMs}} \quad (1)$$

$$BIF_{HAAs} = \frac{C_{BAA} + C_{BCAA} + C_{BDCAA} + 2C_{DBAA} + 2C_{CDBAA} + 3C_{TBAA}}{C_{CAA} + C_{BAA} + 2C_{BCAA} + 2C_{DCAA} + 2C_{DBAA} + 3C_{BDCAA} + 3C_{CDBAA} + 3C_{TCAA} + 3C_{TBAA}} \quad (2)$$

$$BIF_{HANs} = \frac{C_{BAN} + C_{BCAN} + 2C_{DBAN}}{C_{CAN} + C_{BAN} + 2C_{BCAN} + 2C_{DCAN} + 2C_{DBAN} + C_{IAN} + 3C_{TCAN}} \quad (3)$$

$$BIF_{HAMs} = \frac{C_{BAM} + C_{BCAM} + 2C_{DBAM}}{C_{CAM} + C_{BAM} + 2C_{BCAM} + 2C_{DCAM} + 2C_{DBAM} + 3C_{TCAM}} \quad (4)$$

Water sample cytotoxicity after disinfection was investigated. The aggregate cytotoxicity was calculated as was done in previous research (Cuthbertson et al., 2019, 2020; Krasner et al., 2016; Plewa et al., 2017) and with Eq. (5) where the DBP concentrations were divided by their published cytotoxicity concentrations (LC_{50} cytotoxicity values) with the assumption that toxicities are additive. The LC_{50} cytotoxicity values are the DBP concentrations that are associated with a 50% reduction in Chinese hamster ovary cell growth after 72 h of exposure (Table S3) (Plewa et al., 2002, 2008, 2010; Plewa and Wagner., 2009).

$$Calculated\ \text{toxicity}_{DBPs} = \sum_{i=1}^{n} \frac{C_{DBP_i}}{LC_{50_i}} \quad (5)$$

3. Results and discussion

3.1. Effects of disinfection time on DBP formation

3.1.1. Carbonaceous DBPs

Fig. 1a and b show THM and HAA formation in both FBW and SSW increased with longer disinfection contact time. We plot molar, rather than mass concentration units to facilitate comparison among DBP species and to more accurately compare DBP yields (mole DBP per unit DOC) from precursors. Additionally, throughout this work we present the formation of DBPs in undiluted FBW and SSW samples, which is likely to be significantly greater than would be expected at a treatment plant which dilutes FBW and SSW supernatants significantly with plant influent water. However, the precursors present in FBW and SSW samples are chemically unchanged by dilution and thus the trends and potential mitigation strategies identified here are representative of those which would be expected at full-scale. Among four THMs, TCM was the primary THM species in all samples and accounted for 47–60% of the total THM formation. TCM concentrations during chlorination of FBW and SSW reached 358 nM and 387 nM, respectively after a 120 min reaction time. Bromo-THMs (Br-THMs) accounted for 42% and 53% of the total THM yield in FBW and SSW after 120 min., respectively. Br-THMs in SSW were greater than those in FBW due to the greater bromide concentrations in SSW. Br-THMs formed more rapidly than chloro-THMs, reaching 58% at 10 min of their total 120 min formation, compared to chloro-THMs which formed 52% of their total formation at 10 min. Br-THMs are more easily and rapidly generated in the presence of high bromide concentrations because hypobromous acid (HOBr) preferentially substitutes Br atoms more than hypochlorous acid (HOCl) substitutes Cl (Allard et al., 2015; Westerhoff et al., 2004). Although chloro-THMs accounted for greater molar concentrations of the total THM load, Br-THMs should not be ignored given their rapid formation, particularly in cases with high Br^- concentrations.

HAA yields also increased with disinfection time, which was mostly attributed to the increase of chloro-HAAs. CAA concentrations were 45–111 nM in SSW and accounted for 66–76% of the total HAA yield, compared to 12–47% of the HAA yield in FBW attributable to CAA. The difference in CAA concentration is reflective of the overall difference in HAA concentrations, where formation in FBW (30–52 nM) was less than SSW (68–167 nM). This is likely due to lower DOC concentrations in FBW (1.9 compared to 3.1 mgC/L, Table S1). Another reason may be that SSW contained more reactive HAA precursors than FBW (Du et al., 2017; McCormick et al., 2010). In FBW, BCAA was the dominant HAA species within 60 min, but decreased with increasing contact time. HAA may hydrolyze but hydrolysis kinetics are much slower than other DBPs (Wang et al., 2018). However, there was a negative linear correlation between Br-THMs and BCAA in FBW ($R^2 = 0.92$, $p < 0.05$, Fig. S1) indicating that BCAA further reacted with HOBr to form corresponding Br-THMs. Previous research has also determined that HAAs can decompose to THMs (Wang et al., 2019; Zhang and Minear, 2002).

3.1.2. Nitrogenous DBPs

As shown in Fig. 1c, HANs were rapidly generated within the first 10 min and subsequently increased gradually with disinfection time which is attributed to the increased levels of bromo-HANs (Br-HANs). HANs reached their maximum yields at 120 min in FBW and SSW which were 31 and 36 nM, respectively. Among the seven HANs, four HANs (e.g., CAN, DCAN, BCAN and DBAN) were detected

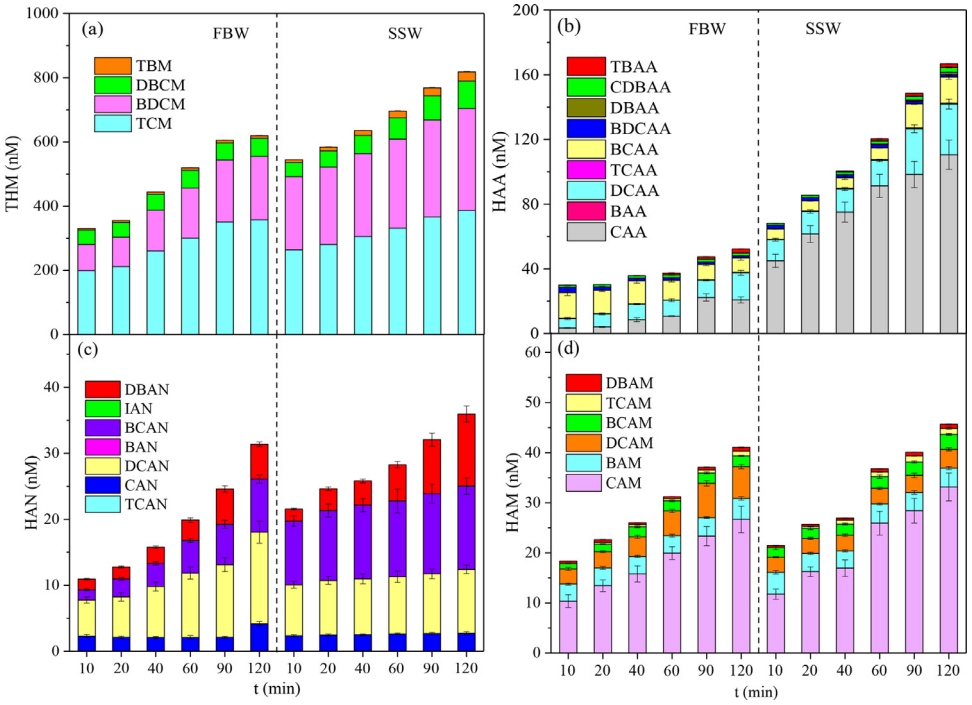

Fig. 1. Effect of disinfectant contact time in FBW or SSW (illustrated as left or right sides of dashed lines) on (a) THM, (b) HAA, (c) HAN, and (d) HAM formation. Experimental conditions: [NaOCl] = 20 mg-Cl_2/L, pH = 7, T = 25±1 °C. Error bars represent one standard deviation of experimental replicates (n = 3).

in FBW and SSW. Br-HANs were the primary HANs in SSW and accounted for 53–66% of the total HAN formation, which contrasted with the formation of HAAs. This result indicated that Br-HANs were generated with increased disinfection times. Br-HANs, especially DBAN, are the most cyto- and genotoxic HANs for which data are available (Wagner and Plewa, 2017). Fig. 1d shows that the total yields of HAMs in FBW and SSW also demonstrated an increasing trend over time which indicated that longer disinfection times enhanced HAM formation. Chloro-HAMs were the main HAM during chlorination. The maximum yields of HAMs in FBW and SSW were observed at 120 min and eventually reached 41 nM and 46 nM, respectively.

In general, total DBP concentrations and calculated toxicities showed a similar trend which increased over time (Figs. S2a and S2c). Although THMs and HAAs predominated among the measured DBP classes at all disinfection times, the calculated toxicities of THMs and HAAs accounted for less than 4% of the total calculated DBPs toxicity due to their low toxic potency (Plewa et al., 2017). Others have also recently shown that THMs are unlikely to be the drivers of toxicity in disinfected samples (Chuang and Mitch, 2017; Li and Mitch, 2018). At low oxidant exposures (*Cxt*, mg-min/L), HAMs are the main DBP that contributed to the calculated toxicity but did not increase over time. The increase in total calculated toxicity is attributed to the increase of HAN formation. HANs constituted 30–53% and 42–66% of the total calculated toxicity, respectively, during FBW and SSW disinfection, and the group toxicity was dominated by DBAN. Therefore, contact times between disinfectant and water should be minimized to reduce DBP formation and associated toxicity.

3.2. Effects of disinfectant dose and type on the DBP formation

3.2.1. Carbonaceous DBPs

The formation of THMs and HAAs in FBW and SSW with 120 min disinfection times at different chlorine and chloramine doses are shown in Fig. 2a and b. The THM yields in both water samples exhibited gradually increasing trends as the chlorine or chloramine doses increased from 5 mg-Cl_2/L to 20 mg-Cl_2/L. THM concentrations in SSW during chlorination were higher than those in FBW due to the high DOC and bromide concentrations in SSW. The maximum yields of THMs in FBW and SSW during chlorination reached 646 nM and 958 nM, respectively, at the highest chlorine dose (20 mg-Cl_2/L). Compared with the chlorination process, THM concentrations in FBW and SSW at a 20 mg-Cl_2/L dose of chloramine decreased by 21% and 50% to 509 nM and 575 nM, respectively. This result showed that THM formation can be effectively controlled by reducing disinfectant dose or by using chloramine as the disinfectant instead of chlorine.

HAA formation was not affected by chlorine dose which was different from THM formation (Fig. 2b). The DCAA and BCAA formations rose continuously with chlorine dose whereas CAA formation had an opposite trend. The reason may be that halogen atoms (Cl and Br) further substituted in the presence of high chlorine doses, so that CAA progressed to form DCAA and BCAA (Wang et al., 2019). In SSW, HAA concentrations decreased by 40–68% during chloramination compared to chlorination, which is attributed to the reduced concentration of CAA. HAA yields were higher at the highest chloramine dose (NH_2Cl concentration = 20 mg-Cl_2/L) than at other doses.

3.2.2. Nitrogenous DBPs

Fig. 2c and d show HANs and HAM formations in FBW and SSW at different chlorine and chloramine doses. The HANs in FBW remained at 31.9 nM to 32.9 nM, respectively, which indicated that the chlorine dose only slightly affected HAN formation. However, HAN yields decreased with increasing chlorine doses in SSW, likely because HANs were hydrolyzed to HAMs or other DBPs (Huang et al., 2012). Previous studies have also reported that HAN degradation rates increased with chlorine concentrations (Chu et al., 2009; Reckhow et al., 2001). As the chloramine dose increased, HAN concentrations reached their maxima at the highest chloramine doses for both water samples. FBW and SSW exhibited the same HAM formation trend during disinfection (Fig. 2d). HAM yields in both water samples decreased as the chlorine dose in-

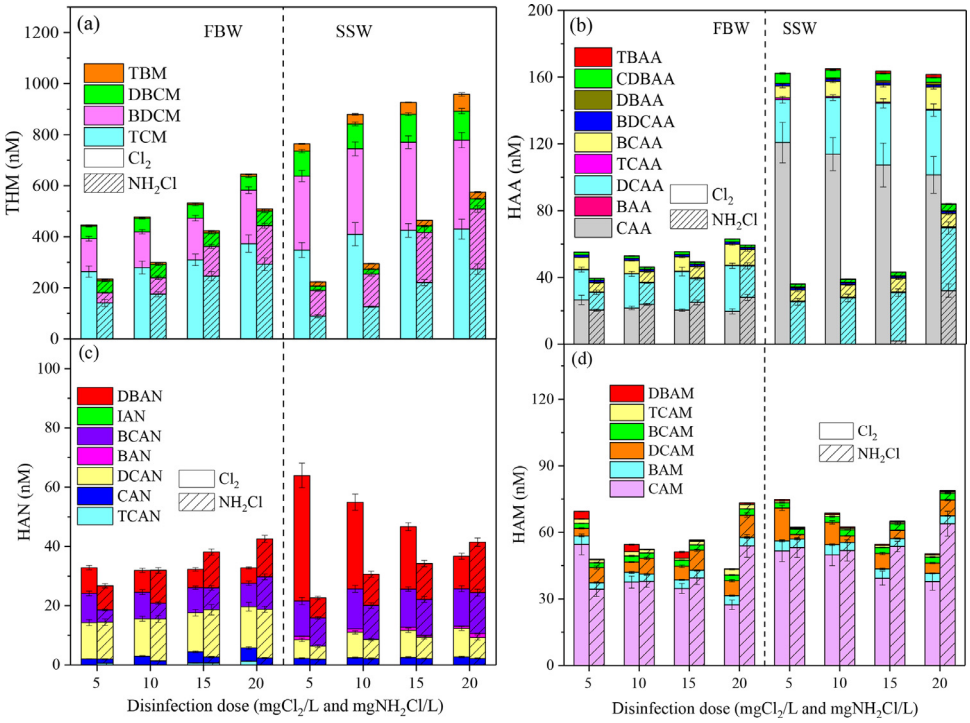

Fig. 2. Effect of disinfectant type and initial dose in FBW or SSW (illustrated as left or right sides of dashed lines) on formation after 120 minutes of reaction time of (a) THM, (b) HAA, (c) HAN, and (d) HAM. Experimental conditions: [NaOCl] and [NH_2Cl] = 5-20 mg-Cl_2/L, pH = 7, T = 25±1 °C. Error bars represent one standard deviation of experimental replicates (n = 3).

creased, which was consistent with the formation of HANs in SSW at different chlorine doses. However, there was an opposite trend of HAM formation during chloramination of both water samples when compared to chlorination, indicating that high chloramine doses favored HAN and HAM formations, consistent with a previous publication (Hong et al., 2013). As shown in Fig. 2c and d, the HAN and HAM concentrations produced by chloramination of FBW and SSW at the highest dose (20 mg-Cl_2/L) exceeded those produced by chlorination. Therefore, DWTPs should focus DBP mitigation efforts on HAN and HAM formation when chloramines are applied to the return flows.

As shown in Fig. S3, the calculated toxicity decreased steadily with increasing chlorine doses which is attributed to the decreased HAN and HAM concentrations. Thus, there may be an opportunity to reduce toxicity by increasing chlorine dose and destroying some more toxic DBPs. This does not however take into account non-detected (i.e., unknown) DBPs, for which the contribution to total toxicity is likewise unknown, but may be substantial (McKenna et al., 2020; Stalter et al., 2020). In both samples and at the highest chlorine/chloramine dose, calculated toxicities with chloramination exceeded those at the highest chlorine dose. Thus, minimizing chloramine dose or use of free chlorine may be preferential to control DBP formation in situation with recycling of SSW and FBW.

3.3. Effects of pH on DBP formation during chlorination

3.3.1. Carbonaceous DBPs

The formation of THMs and HAAs in FBW and SSW at varying pH are shown in Fig. 3a and b. The THM and HAA yields in FBW and SSW gradually increased as the pH increased from 6 to 8. This is because THM and HAA formation by base-catalyzed hydrolysis prevails under alkaline conditions (Liang and Singer, 2003). During SSW chlorination, the maximum THM and HAA formation were higher than those of FBW, and reached 1,072 nM and 198 nM, respectively at pH 8. Among four THMs and nine HAAs, TCM and CAA were affected the most by pH. Moreover, BDCM and DBAM yields also increased with increasing pH and these results agree with previous studies which showed that alkaline environments favor formation of THMs and HAAs (Fang et al., 2019).

3.3.2. Nitrogenous DBPs

HANs exhibited a trend that was opposite to THMs and HAAs, such that HANs were produced to a greater extent at acidic and neutral conditions compared to alkaline conditions (Fig. 3c). These results are consistent with previous studies showing that HAN hydrolysis increases with pH (Reckhow et al., 2001; Yu and Reckhow, 2015). Previous studies have also determined that HAN yields reached peaks at pH 7 for some model precursors (Fang et al., 2019).

HAM formation steadily decreased from 57 nM to 14 nM in FBW, and from 61 nM to 34 nM in SSW, as the pH increased from 6 to 8. Both HAMs and HANs hydrolyze under alkaline conditions, eventually to the corresponding HAAs. Although hydrolysis of HANs to HAMs should increase measured HAM concentrations (Ding et al., 2018; Huang et al., 2013; Yu and Reckhow, 2017), it is likely that the corresponding HAM hydrolyzed to HAAs before measurement and instead account for some formation of measured HAAs.

Hydrolysis of HAMs and HANs to HAAs is notable because nitrogenous DBPs are generally more toxic than carbonaceous (Wagner and Plewa, 2017). In Fig. S4 we show the calculated toxicities after chlorination of both water samples versus pH. Total DBP formation increased with increasing pH but calculated DBP toxicity deceased steadily due to minimization of HAN and HAMs. The unadjusted pH of the FBW and SSW samples was 7.5 and 7.7 (Table S1), however, FBW and SSW are typically recycled to the head of the plant and thus are subject to chlorination at the pH of the finished water. Thus, pH at the point of chlorination and in the distribution system should be monitored and adjusted to increase hydrolysis of HAMs and HANs. Again, this is based on the toxicity

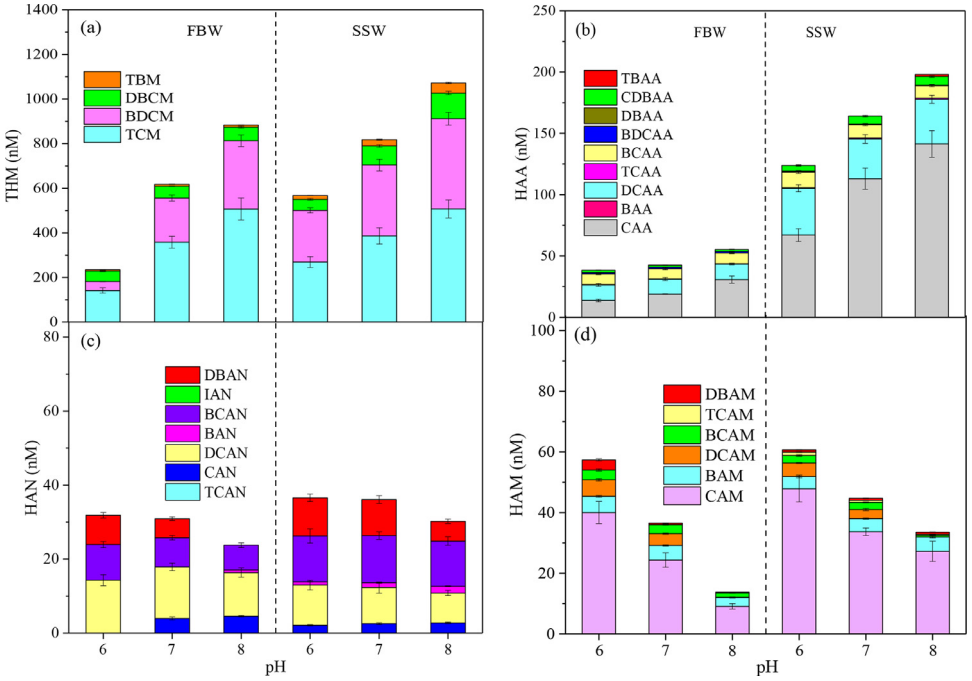

Fig. 3. Effect of pH values in FBW or SSW (illustrated as left or right sides of dashed lines) on formation of (a) THM, (b) HAA, (c) HAN, and (d) HAM. Experimental conditions: [NaOCl] = 20 mg-Cl_2/L, reaction time = 120 min, T = 25±1 °C. Error bars represent one standard deviation of experimental replicates (n = 3).

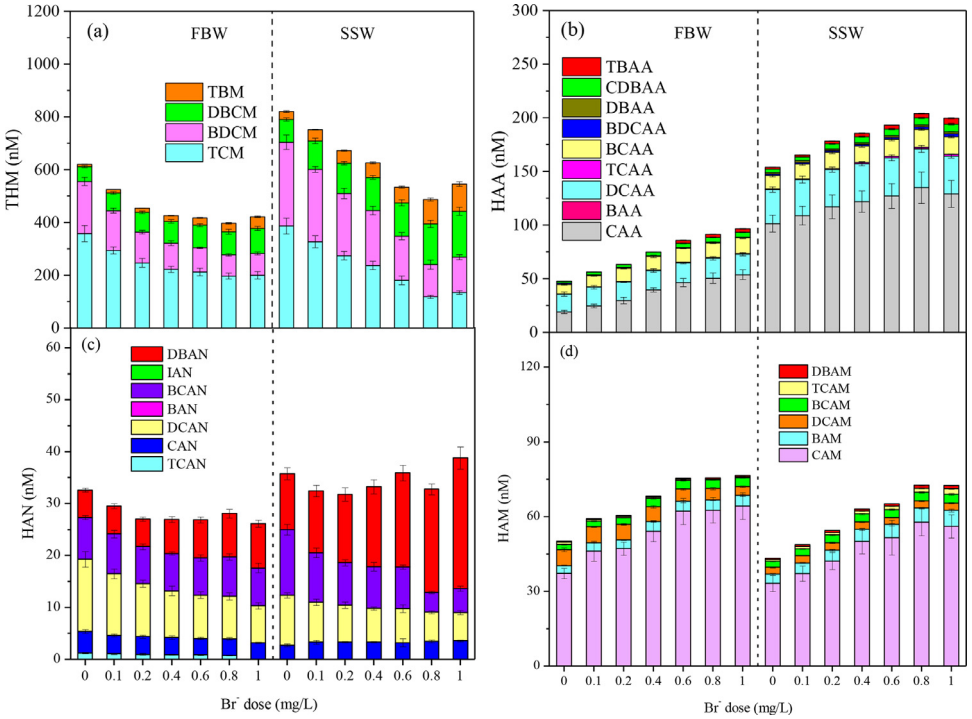

Fig. 4. Effect of bromide concentrations in FBW or SSW (illustrated as left or right sides of dashed lines) on formation of (a) THM, (b) HAA, (c) HAN, and (d) HAM. Experimental conditions: [NaOCl] = 20 mg-Cl_2/L, pH = 7, reaction time = 120 min, T = 25±1 °C. Error bars represent one standard deviation of experimental replicates (n = 3).

of the measured DBPs, which does not encompass all potentially toxic organic matter in the chlorinated samples.

3.4. Effect of bromide on the DBP formation during chlorination

3.4.1. Carbonaceous DBPs

As shown in Fig. 4a, THM formation decreased at bromide additions between 0 mg/L and 0.8 mg/L, followed by an increase with addition of 1 mg/L bromide. THM formation tended to decrease with increasing dose due to the decrease of TCM and BDCM formation. As bromide levels increased, DBCM formation also gradually increased from 56 nM to 95 nM and from 9 nM to 44 nM in FBW and SSW, respectively. TBM formation increased at greater doses of bromide, from 86 nM to 174 nM and from 30 nM to 103 nM, for FBW and SSW, respectively. However, the sum of the in-

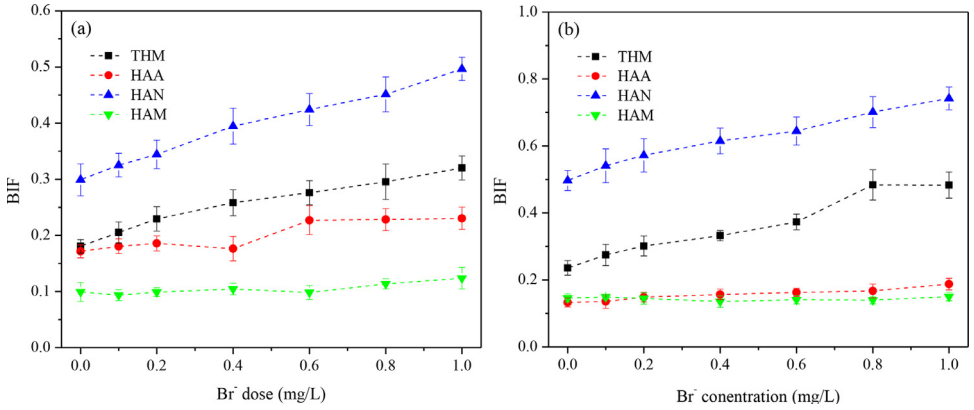

Fig. 5. BIF for (a) FBW and (b) SSW waters oxidized at differing initial bromide concentrations. Experimental conditions: [NaOCl] = 20 mg-Cl_2/L, pH = 7, reaction time = 120 min, T = 25±1 °C. Error bars represent one standard deviation of experimental replicates (n = 3).

crease of DBCM and TBM was lower than the losses of TCM and BDCM indicating that the increase in more brominated THMs was due partially to oxidation of additional organic matter rather than further oxidation of lesser brominated THMs. BIF values for THMs in both water sources also continuously increased (Fig. 5a).

HAA formation during chlorination of both water samples at different bromide doses increased with bromide concentrations due mostly to increased CAA formation. DCAA, BCAA, CDBAA and TBAA also slightly increased with bromide concentrations. With increasing bromide, BIF was modestly increased, to much less of an extent than for THMs, illustrating that THMs are more subject to bromine substitution than HAAs.

3.4.2. Nitrogenous DBPs

The total HAN formation during chlorination of FBW and SSW remained relatively stable with increasing bromide doses (from 26 nM to 33 nM in FBW and from 32 nM to 39 nM in SSW (Fig. 4c)). DCAN formation was decreased to the greatest extent at higher bromide doses (decreased in FBW and SSW from 14 nM to 7 nM and from 10 nM to 6 nM, respectively) but was offset by the formation of DBAN. DBAN formation increased from 5 nM to 9 nM and from 11 nM to 25 nM, respectively. A total bromide (spiked plus background) concentration of 0.4 mg/L was the inflection point where Br-HANs began to dominate the HAN pool over chloro-HANs.

Similar to the formation of HAAs, HAM formation increased with bromide, although a plateauing was apparent at bromide concentrations above 0.65 mg/L (FBW) and 1.22 mg/L (SSW). The reason for this plateauing is not clear but the maximum formations of HAMs in FBW and SSW were found at the highest bromide dose and reached 76 nM and 73 nM, respectively.

The BIF values of HANs for both water samples all rose noticeably with increasing bromide concentrations and exhibited the greatest BIF values among the four measured DBPs (Fig. 5). The greater incorporation of bromide into HANs is consistent with published literature (Fang et al., 2019). HAM BIF did not increase with increasing bromide dose.

Total DBP concentrations and calculated toxicities from the chlorination of both water samples at varying bromide dose are shown in Fig. S5. THM concentrations were much greater than any other group of DBP. However, increasing calculated toxicity as a function of bromide dose is attributable to increasing formation of DBAN and CAM rather than THMs. HANs accounted for 3.2–4.7% of the total DBPs but contributed 54–68% of the calculated toxicity. Therefore, strategies for bromide removal from FBW and SSW should be considered to reduce DBP formation, especially bromo-DBPs, during FBW and SSW recycling.

4. Conclusion

This study investigated the formation of THMs, HAAs, HANs and HAMs during disinfection of FBW and SSW and specific conclusions are as follows:

(1) When pH, disinfectant concentration, and bromide concentrations were held constant, nearly all detected DBP concentrations increased with increasing contact time. Calculated toxicity also tended to increase with increasing chlorine contact time.
(2) Reducing chlorine dose reduced THM formation but promoted HAN and HAM formation, resulting in increased calculated toxicity. For chloramination of FBW and SSW, formation of N-DBPs was greatest at the highest applied chloramine dose.
(3) Alkaline pH effectively controlled N-DBP formation but increased C-DBP formation likely due to hydrolysis of the N-DBPs. Hydrolysis of the more toxic N-DBPs reduced calculated toxicity.
(4) BIFs for THMs and HANs increased with increasing bromide concentration, but were relatively constant for HAAs and HAMs. Increasing bromide concentrations caused an increased in calculated toxicity due mostly to the formation of DBAN.
(5) Reducing disinfection contact time, increasing chlorine dose or decreasing chloramine dose, and removing bromide from FBW and SSW are effective strategies for reducing DBP formation and the calculated toxicity of THMs, HANs, HAAs, and HAMs during FBW and SSW recycling.
(6) Hydrolysis of DBPs via pH control may be an effective strategy in reducing risk to consumers

Declaration of Competing Interest

The authors declare that they have no known competing financial interests or personal relationships that could have appeared to influence the work reported in this paper.

Acknowledgments

This research is partially supported by the National Science Foundation (CBET-1804229; CBET-1804255; EEC-1449500) and Water Research Foundation (Projects #4711 and #5005). This study was also supported by the National Natural Science Foundation of China (NSFC 22076026, 21777031, 21577024).

Supplementary materials

Supplementary material associated with this article can be found, in the online version, at doi:10.1016/j.watres.2021.116964.

References

Allard, S., Tan, J., Joll, C.A., Gunten, U.V., 2015. Mechanistic study on the formation of Cl-/Br-/I-trihalomethanes during chlorination/chloramination combined with a theoretical cytotoxicity evaluation. Environ. Sci. Technol. 49 (18), 11105–11114.

An, D., Chen, Y.N., Gu, B., Westerhoff, P., Hanigan, D., 2019. Lower molecular weight fractions of PolyDADMAC coagulants disproportionately contribute to N-nitrosodimethylamine formation during water treatment. Water Res. 150, 466–472.

An, D., Gu, B., Sun, S.N, Zhang, H., Chen, Y.N, Zhu, H.F, Shi, J., Tong, J., 2017. Relationship between THMs/NDMA formation potential and molecular weight of organic compounds for source and treated water in Shanghai. China. Sci. Total Environ. 605–606, 1–8.

APHA, A., Water Environment Federation, 2005. Standard Methods for the Examination of Water and Wastewater, Twenty-Firsted. APHA, Washington DC, USA.

Bond, T., Huang, J., Templeton, M.R., Graham, N., 2011. Occurrence and control of nitrogenous disinfection by-products in drinking water – a review. Water Res. 45, 4341–4354.

Bourgeois, J.C., Walsh, M.E., Gagnon, G.A., 2004. Comparison of process options for treatment of water treatment residual streams. J. Environ. Eng. Sci. 3 (6), 477–484.

California Department of Public Health, 2013. NDMA and Other Nitrosamines-Drinking Water Issues.

Cantor, K.P., Villanueva, C.M., Silverman, D.T., Figueroa, J.D., Real, F.X., Garcia-Closas, M., Malats, N., Chanock, S., Yeager, M., Tardon, A., Garcia-Closas, R., Serra, C., Carrato, A., Castano-Vinyals, G., Samanic, C., Rothman, N., Kogevinas, M., 2010. Polymorphisms in GSTT1, GSTZ1, and CYP2E1, disinfection by-products, and risk of bladder cancer in Spain. Environ. Health Perspect. 118, 1545–1550.

Chu, W.H., Gao, N.Y., Deng, Y., 2009. Stability of new found nitrogenous disinfection by-products haloacetamides in drinking water. Chin. J. Org. Chem. 29, 1569–1574.

Chuang, Y.H., Mitch, W.A., 2017. Effect of ozonation and biological activated carbon treatment of wastewater effluents on formation of N-nitrosamines and halogenated disinfection byproducts. Environ. Sci. Technol. 51 (4), 2329–2338.

Chuang, Y.H., Szczuka, A., Mitch, W.A., 2019. Comparison of toxicity-weighted disinfection byproduct concentrations in potable reuse waters and conventional drinking waters as a new approach to assessing the quality of advanced treatment train waters. Environ. Sci. Technol. 53, 3729–3738.

Costet, N., Villanueva, C.M., Jaakkola, J.J.K., Kogevinas, M., Cantor, K.P., King, W.D., Lynch, C.F., Nieuwenhuijsen, M.J., Cordier, S., 2011. Water disinfection by-products and bladder cancer: is there a European specificity? A pooled and meta–analysis of European caseecontrol studies. Occup. Environ. Med. 68, 379.

Cuthbertson, A.A., Kimura, S.Y., Liberatore, H.K., Knappe, D.R.U., Stanford, B.D., Summers, R.S., Dickenson, E.R., Maness, J.C., Glover, C., Selbes, M., Richardson, S.D., 2020. GAC to BAC: does it make chloraminated drinking water safer? Water Res. 172, 115432–115443.

Cuthbertson, A.A., Kimura, S.Y., Liberatore, H.K., Summers, R.S., Knappe, D.R.U., Stanford, B.D., Maness, J.C., Mulhern, R.E., Selbes, M., Richardson, S.D., 2019. Does granular activated carbon with chlorination produce safer drinking water? From disinfection byproducts and total organic halogen to calculated toxicity. Environ. Sci. Technol. 53, 5987–5999.

Ding, S.K., Chu, W.H., Krasner, S.W., Yu, Y., Fang, C., Xu, Bin., Gao, N.Y., 2018. The stability of chlorinated, brominated, and iodinated haloacetamides in drinking water. Water Res. 142, 490–500.

Du, Y., Lv, X.T., Wu, Q.Y., Zhang, D.Y., Zhou, Y.T., Peng, L., Hu, H.Y., 2017. Formation and control of disinfection byproducts and toxicity during reclaimed water chlorination: a review. Water Res. 58, 51–63.

Fang, C., Hu, J.L., Chu, W.H., Ding, S.K., Zhao, T.T., Lu, X.Y., Zhao, H.Y., Yin, D.Q., Gao, N.Y., 2019. Formation of CX_3R-type disinfection by-products during the chlorination of protein: The effect of enzymolysis. Chem. Eng. J. 363, 309–317.

Gottfried, A., Shepard, A.D., Hardiman, K., Walsh, M.E., 2008. Impact of recycling filter backwash water on organic removal in coagulation–sedimentation processes. Water Res. 42 (18), 4683–4691.

Guay, C., Rodriguez, M., Serodes, J., 2005. Using ozonation and chloramination to reduce the formation of trihalomethanes and haloacetic acids in drinking water. Desalination 176 (1-3), 229–240.

Hanigan, D., Truong, L., Simonich, M., Tanguay, R., Westerhoff, P., 2017. Zebrafish embryo toxicity of 15 chlorinated, brominated, and iodinated disinfection by-products. J. Environ Sci. 58, 302–310.

Hanigan, D., Zhang, J., Herckes, P., Zhu, E., Krasner, S.W., Westerhoff, P., 2015. Contribution and removal of watershed and cationic polymer N-nitrosodimethylamine precursors. J. Am Water Works Ass. 107 (3), 152–163.

Hong, B.W., Lin, T., Chen, W., 2016. Evaluation of a drinking water treatment process involving directly recycling filter backwash water using physico-chemical analysis and toxicity assay. RSC Adv. 6, 76922–76933.

Hong, H.C., Xiong, Y.J., Ruan, M.Y., Liao, F.L., Lin, H.J., Liang, Y., 2013. Factors affecting THMs, HAAs and HNMs formation of Jin Lan reservoir water exposed to chlorine and monochloramine. Sci. Total Environ. 44, 196–204.

Hua, G., Reckhow, D.A., 2007. Comparison of disinfection byproduct formation from chlorine and alternative disinfectants. Water Res. 41, 1667–1678.

Huang, H., Wu, Q.Y., Hu, H.Y., Mitch, W.A., 2012. Dichloroacetonitrile and dichloroacetamide can form independently during chlorination and chloramination of drinking waters, model organic matters, and wastewater effluents. Environ. Sci. Technol. 46 (19), 10624–10631.

Huang, H., Wu, Q.Y., Tang, X., Jiang, R., Hu, H.Y., 2013. Formation of haloacetonitriles and haloacetamides during chlorination of pure culture bacteria. Chemosphere 92, 375–381.

Jones, D.B., Saglam, A., Triger, A., Song, H., Karanfil, T., 2011. I-THM formation and speciation: preformed monochloramine versus prechlorination followed by ammonia addition. Environ. Sci. Technol. 45, 10429–10437.

King, J.F., Szczuka, A., Zhang, Z., Mitch, W.A., 2020. Efficacy of ozone for removal of pesticides, metals and indicator virus from reverse osmosis concentrates generated during potable reuse of municipal wastewaters. Water Res. 176, 115744–115754.

Krasner, S.W., Mitch, W.A., McCurry, D.L., Hanigan, D., Westerhoff, P., 2013. Formation, precursors, control, and occurrence of nitrosamines in drinking water: a review. Water Res. 47 (13), 4433–4450.

Krasner, S.W., Lee, T.C.F., Westerhoff, P., Fischer, N., Hanigan, D., Karanfil, T., Wilson, B.S., Liz, T.E., Andrews, R.C., 2016. Granular activated carbon treatment may result in higher predicted genotoxicity in the presence of bromide. Environ. Sci. Technol. 50 (17), 9583–9591.

Krasner, S.W., Westerhoff, P., Chen, B., Rittmann, B.E., Amy, G., 2009. Occurrence of disinfection byproducts in United States wastewater treatment plant effluents. Environ. Sci. Technol. 43 (21), 8320–8325.

Krasner, S.W., Westerhoff, P., Mitch, W.A., Hanigan, D., McCurry, D.L., Von Gunten, U., 2018. Behavior of NDMA precursors at 21 full-scale water treatment facilities. Environ. Sci-Wat. Res. 4 (12), 1966–1978.

Lau, S.S., Wei, X., Bokenkamp, K., Wagner, E.D., Mitch, W.A., 2020. Assessing additivity of cytotoxicity associated with disinfection byproducts in potable reuse and conventional drinking waters. Environ. Sci. Technol. 54 (9), 5729–5736.

Li, X.F., Mitch, W.A., 2018. Drinking water disinfection byproducts (DBPs) and human health effects: multidisciplinary challenges and opportunities. Environ. Sci. Technol. 52 (4), 1681–1689.

Liang, L., Singer, P.C., 2003. Factors influencing the formation and relative distribution of haloacetic acids and trihalomethanes in drinking water. Environ. Sci. Technol. 37, 2920–2928.

Massachusetts Office of Energy and Environmental Affairs (EEA), 2004. Current Regulatory Limit: N-Nitrosodimethylamine (NDMA).

McCormick, N.J., Porter, M., Walsh, M.E., 2010. Disinfection by-products in filter backwash water: implications to water quality in recycle designs. Water Res. 44, 4581–4589.

McKenna, E., Thompson, K.A., Taylor-Edmonds, L., McCurry, D.L., Hanigan, D., 2020. Summation of disinfection by-product cho cell relative toxicity indices: sampling bias, uncertainty, and a path forward. Environ. Sci.-Proc. Imp. 22 (3), 708–718.

Muellner, M., Wagner, E., McCalla, K., Richardson, S., Woo, Y., Plewa, M.J., 2007. Haloacetonitriles vs. regulated haloacetic acids: are nitrogen-containing DBPs more toxic? Environ. Sci. Technol. 41 (2), 645–651.

Petronijevic, M., Agbaba, J., Razic, S., Molnar Jazic, J., Tubic, A., Watson, M., Dalmacija, B., 2019. Fate of bromine-containing disinfection by-products precursors during ozone and ultraviolet-based advanced oxidation processes. Int. J. Environ. Sci. Technol. 16 (1), 171–180.

Plewa, M.J., Kargalioglu, Y., Vankerk, D., Minear, R.A., Wagner, E.D., 2002. Mammalian cell cytotoxicity and genotoxicity analysis of drinking water disinfection by-products. Environ. Mol. Mutagen. 40, 134–142.

Plewa, M.J., Muellner, M.G., Richardson, S.D., Fasano, F., Buettner, K.M., Woo, Y.T., McKague, A.B., Wagner, E.D., 2008. Occurrence, synthesis, and mammalian cell cytotoxicity and cenotoxicity of haloacetamides: an emerging class of nitrogenous drinking water disinfection byproducts. Environ. Sci. Technol. 42 (3), 955–961.

Plewa, M.J., Simmons, J.E., Richardson, S.D., Wagner, E.D., 2010. Mammalian cell cytotoxicity and genotoxicity of the haloacetic acids, a major class of drinking water disinfection by-products. Environ. Mol. Mutagen. 51, 871–878.

Plewa, M.J., Wagner, E.D., 2009. Mammalian Cell Cytotoxicity and Genotoxicity of Disinfection By-Products. Water Research Foundation, Denver, CO, p. p134.

Plewa, M.J., Wagner, E.D., Richardson, S.D., 2017. TIC-Tox: a preliminary discussion on identifying the forcing agents of DBP-mediated toxicity of disinfected water. J. Environ. Sci. 58, 208–216.

Qian, Y.K., Hu, Y., Chen, Y.N., An, D., Westerhoff, P., Hanigan, D., Chu, W.H., 2020. Haloacetonitriles and haloacetamides precursors in filter backwash and sedimentation sludge water during drinking water treatment. Water Res. 186, 116346.

Rahman, M.B., Driscoll, T., Cowie, C., Armstrong, B.K., 2010. Disinfection by-products in drinking water and colorectal cancer: a meta-analysis. Int. J. Epidemiol. 39, 733–745.

Reckhow, D.A., Platt, T.L., Macneill, A.L., Mcclellan, J.N., 2001. Formation and degradation of dichloroacetonitrile in drinking waters. J. Water Supply Res. T 50, 1–13.

Richardson, S.D., Plewa, M.J., Wagner, E.D., Schoeny, R., DeMarini, D.M., 2007. Occurrence, genotoxicity, and carcinogenicity of regulated and emerging disinfection by-products in drinking water: a review and roadmap for research. Mutat. Res., Rev. Mutat. Res. 636 (1–3), 178–242.

Sedlak, D.L., Gunten, U.V., 2011. The chlorine dilemma. Science 331, 42–43.

Shannon, M.A., Bohn, P.W., Elimelech, M., Georgiadis, J.G., Marinas, B.J., Mayes, A.M., 2008. Science and technology for water purification in the coming decades. Nature 452, 301–310.

Stalter, D., O'Malley, E., Gunten, U.V., Escher, B.I., 2020. Mixture effects of drinking water disinfection by-products: implications for risk assessment. Environ. Sci.-Water Res. 6 (9), 2341–2351.

Standardization Administration of the People's Republic of China, 2006. GB 5749-2006 standards for drinking water quality.

U.S. EPA,1995. Method 551.1: determination of chlorination disinfection byproducts chlorinated solvents, and halogenated pesticides/herbicides in drinking water by liquid-liquid extraction and gas chromatography with electron capture detection.

U.S. EPA, 2003. Method 552.3: Determination of Haloacetic Acid and Dalapon in Drinking Water by Liquid-Liquid Extraction, Derivatization, and Gas Chromatography with Electron Capture Detection. Revision 1.0; Technical Support Center. Office of Ground Water and Drinking Water. U.S. Environmental Protection Agency, Cincinnati, OHIO.

U.S. EPA, 2006. Stage 2 disinfectants and disinfection byproducts rule: national primary and secondary drinking water regulations: final rule. Federal Register 71.

Verdugo, E.M., Gifford, M., Glover, C., Cuthbertson, A.A., Trenholm, R.A., Kimura, S.Y., Liberatore, H.K., Richardson, S.D., Stanford, B.D., Summers, R.S., Dickenson, E.R.V., 2020. Controlling disinfection byproducts from treated wastewater using adsorption with granular activated carbon: impact of pre-ozonation and pre-chlorination. Water Res. X 9, 100068.

Villanueva, C.M., Cantor, K.P., Cordier, S., Jaakkola, J., King, W.D., Lynch, C., Porru, S., Kogevinas, M., 2004. Disinfection byproducts and bladder cancer: a pool analysis. Epidemiology 15, 357–367.

Villanueva, C.M., Cantor, K.P., Grimalt, J.O., Malats, N., Silverman, D., Tardon, A., Garcia-Closas, R., Serra, C., Carrato, A., Castaño-Vinyals, G., Marcos, R., Rothman, N., Real, F.X., Dosemeci, M., Kogevinas, M., 2006. Bladder cancer and exposure to water disinfection by-products through ingestion, bathing, showering, and swimming in pools. Am. J. Epidemiol. 165 (2), 148–156.

Vu, T.N., Kimura, S.Y., Plewa, M.J., Richardson, S.D., Mariñas, B.J., 2018. Predominant N-haloacetamide and haloacetonitrile formation in drinking water via the aldehyde reaction pathway. Environ. Sci. Technol. 53 (2), 850–859.

Wagner, E.D., Plewa, M.J., 2017. CHO cell cytotoxicity and genotoxicity analyses of disinfection by-products: an updated review. J. Environ. Sci. 58, 64–76.

Wang, L., Chen, B., Zhang, T., 2018. Predicting hydrolysis kinetics for multiple types of halogenated disinfection byproducts via QSAR models. Chem. Eng. J. 342, 372–385.

Wang, J., Gong, T., Xian, Q., 2019. Formation of haloacetic acids from different organic precursors in swimming pool water during chlorination. Chemosphere 247, 125793.

Westerhoff, P., Chao, P., Mash, H., 2004. Reactivity of natural organic matter with aqueous chlorine and bromine. Water Res. 38 (6), 1502–1513.

Westerhoff, P., Herckes, P., Fischer, N., Donovan, S., Atkinson, A., Corwell, D., Brown, R., Croue, J.P., Linge, K.L., Liew, D., Lowe, A., 2019. Understanding the Source and Fate of Polymer-Derived Nitrosamine Precursors. Water Research Foundation, Denver, p. 174.

WHO, 2008. N-Nitrosodimethylamine in Drinking-water. Background Document for Development of WHO Guidelines for Drinking-water Quality. World Health Organization.

Yang, X., Shang, C., Westerhoff, P., 2007. Factors affecting formation of haloacetonitriles, haloketones, chloropicrin and cyanogen halides during chloramination. Water Res. 41, 1193–2000.

Yu, Y., Reckhow, D.A., 2015. Kinetic analysis of haloacetonitrile stability in drinking waters. Environ. Sci. Technol. 49, 11028–11036.

Yu, Y., Reckhow, D.A., 2017. Formation and occurrence of N-chloro-2,2-dichloroacetamide, a previously overlooked nitrogenous disinfection byproduct in chlorinated drinking waters. Environ. Sci. Technol. 51, 1488–1497.

Zeng, T., Plewa, M.J., Mitch, W.A., 2016. N-Nitrosamines and halogenated disinfection byproducts in U.S. full advanced treatment trains for potable reuse. Water Res. 101, 176–186.

Zhang, A.H., Wang, F.F., Chu, W.H., Yang, Xu., Pan, Y., Zhu, H.F., 2019. Integrated control of CX_3R-type DBP formation by coupling thermally activated persulfate pre-oxidation and chloramination. Water Res. 160, 304–312.

Zhang, X., Minear, R.A., 2002. Decomposition of trihaloacetic acids and formation of the corresponding trihalomethanes in drinking water. Water Res. 36 (14), 3665–3673.